In Combinatorial Image Analysis, Springer LNCS 4040, R. Reulke et al. (Eds.), pp. 263-276, Berlin, Germany, June 2006

A Comparison of Shape Matching Methods for Contour Based Pose Estimation*

Bodo Rosenhahn[1], Thomas Brox[2], Daniel Cremers[2], and Hans-Peter Seidel[1]

[1] MPI for Informatics, Stuhlsatzenhausweg 85
66123 Saarbrücken, Germany
{rosenhahn,hpseidel}@mpi-inf.mpg.de

[2] CVPR Group, University of Bonn, Römerstr. 164, 53117 Bonn, Germany
{brox,dcremers}@cs.uni-bonn.de

Abstract. In this paper, we analyze two conceptionally different approaches for shape matching: the well-known iterated closest point (ICP) algorithm and variational shape registration via level sets. For the latter, we suggest to use a numerical scheme which was introduced in the context of optic flow estimation. For the comparison, we focus on the application of shape matching in the context of pose estimation of 3-D objects by means of their silhouettes in stereo camera views. It turns out that both methods have their specific shortcomings. With the possibility of the pose estimation framework to combine correspondences from two different methods, we show that such a combination improves the stability and convergence behavior of the pose estimation algorithm.

1 Introduction

Shape matching or shape registration is the basis for many computer vision techniques, such as image segmentation, pose estimation, and image retrieval, to name only few of them. As a consequence, a multitude of works on shape matching can be found in the literature, e.g., [4, 25, 11, 23, 14, 17]; see [24] for a survey.

Most of these approaches rely on classic explicit shape representations given by points that can be connected by lines or higher order curve segments to form a shape. A very popular shape matching method working on such representations is the iterated closest point (ICP) algorithm [2], at which we will take a closer look in Section 2.

An alternative to explicit shape models emerged in the form of implicit representations by means of level sets [10, 16]. Instead of representing a 2-D shape by the points on its contour, the contour is constituted implicitly by the zero-level line of a 2-D embedding function. Level set methods enjoy great popularity in the context of image segmentation with active contours. Recent methods in this field improve the results by integrating the knowledge of previously learned shapes

* We gratefully acknowledge funding by the DFG project CR250/1 and the Max-Planck Center for visual computing and communication.

[15], which involves matching the learned shape representation to the shape that is found in the image. Shape matching with level set representations has been suggested in this context by [15, 17, 9, 19]. In Section 3, we are concerned with such implicit shape representations and propose a numerical scheme from optic flow estimation for matching. In comparison to previous numerics in this field, this matching scheme ensures stability and provides a significant speedup.
Since the two mentioned classes of shape matchers are based on very different concepts, the question of superiority of the one or the other arises.[1] We have therefore compared both approaches in the case of one prominent application, namely silhouette based 2-D-3-D pose estimation. The relevance of shape matching in this context is briefly described in Section 4. The comparison in Section 5 shows that both matching concepts have their pros and cons. By a combination one can, at least in the context of silhouette based pose estimation, obtain the best of both approaches. The paper is concluded by a summary in Section 6.

2 Shape Matching with ICP

The goal of shape registration can be formulated as follows: Given two shapes and a distance measure, the task is to determine from a certain class of transformations one that leads to the minimum distance between the two shapes. The original ICP algorithm registers two point sets P and Q provided $TP \subseteq Q$ with the transformation T being a rigid transformation:

1. **Nearest point search**: for each point $p \in P$ find the closest point $q \in Q$.
2. **Compute registration**: determine the transformation T that minimizes the sum of squared distances between pairs of closest points (p, q).
3. **Transform**: apply the transformation T to all points in set P.
4. **Iterate**: repeat step 1 to 3 until the algorithm converges.

This algorithm converges to the next local minimum of the sum of squared distances between closest points. A good initial estimate is required to ensure convergence to the sought solution. Unwanted solutions may be found, if the sought transformation is too large, e.g. many shapes have a convergence radius in the area of 20° [7], or if the point sets do not provide sufficient information for a unique solution.
The original ICP algorithm has been modified in order to improve the rate of convergence and to register partially overlapping point sets. Zhang [25] uses a modified cost function based on robust statistics to limit the influence of outliers. The work also suggests to use a K-dimensions tree to partition the point set and the author further reports on a significant speedup when registering large

[1] We want to note here that the ICP algorithm can also match surfaces and, hence, could as well be used to match implicit contours represented by level sets (which are surfaces, in fact). The focus of our comparison is on explicit and implicit contour representations. We take here the ICP algorithm as a representative for matching methods that work with explicit contours. Consequently, *ICP* has to be interpreted in this paper as *ICP with an explicit contour representation*.

range image data sets. Bergevin et al. [1] extended the ICP algorithm to range images from multiple views. They ensure an even distribution of registration errors between overlapping views and report errors less than the range image measurement noise for multiple views of complex objects.
The accuracy of ICP depends on the *geometric information* (e.g. local curvatures) contained in the point sets. If insufficient shape information is available, inaccurate or incorrect registration may occur. Pennec et al. [18] developed a framework to characterize the uncertainty in point registration. Other approaches aim at the avoidance of local minima during registration subsuming the use of Fourier descriptors [21], color information [13], or curvature features [22].
The advantages of ICP algorithms are obvious: they are easy to implement and will provide good results, if the sought transformation is not too large. ICP algorithms have also been used for silhouette based 2D-3D pose estimation [20, 21]. In this context, additional problems arise due to ambiguities of transformations in direction of the projection rays. Sampling methods can be used to avoid some of these additional local optima, yet this is usually a very time consuming procedure.

3 Shape Matching with Level Sets and Optic Flow

3.1 Shape Representation with the Euclidean Distance Transform

In contrast to the point sets used for ICP algorithms, the method suggested in this section deals with shapes represented by an embedding function $\Phi : \Omega \subset \mathbb{R}^2 \rightarrow \mathbb{R}$. The contour can be obtained from such a representation as the zero-level line $C := \{\mathbf{x} \in \Omega | \Phi(\mathbf{x}) = 0\}$.
For a given contour, the representation by an embedding function is not unique. In general, one sets the values of Φ to the signed Euclidean distance of the next contour point

$$\Phi(\mathbf{x}) = \begin{cases} D(\mathbf{x}, C) & \mathbf{x} \text{ inside } C \\ -D(\mathbf{x}, C) & \mathbf{x} \text{ outside } C \\ 0 & \mathbf{x} \in C \end{cases} \tag{1}$$

where $D(\mathbf{x}, C)$ denotes the Euclidean distance of $x \in \Omega$ to the closest point $\tilde{\mathbf{x}}$ on the contour C. This choice of Φ has, among others, the nice property of being invariant under rotation and translation. It can be efficiently computed from a binary shape image by the algorithm given in [12]. The distance functions of two shapes are shown in Fig. 1.
Although the embedding of a shape in a higher dimensional space appears, on the first glance, to be less efficient than explicit representations, a closer look reveals many advantages. One such advantage is the flexibility of implicit shapes concerning their topology. While many explicit shape representations induce problems when a shape consists of several parts or contains enclosures, such cases are naturally handled in the level set framework.

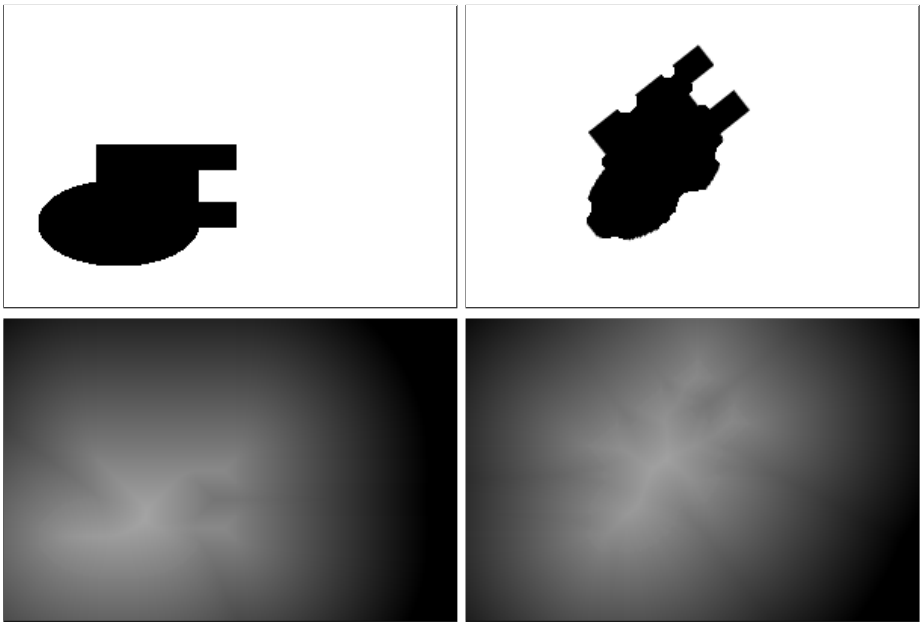

Fig. 1. Top: Source and target shapes that are to be matched. **Bottom:** Euclidean distance functions Φ of these shapes shown by gray value images in the range $[0, 255]$ where 128 marks the zero-level of Φ, i.e., dark areas show negative values of Φ, bright areas show positive values.

A straightforward distance measure for shapes being represented by embedding functions Φ_1 and Φ_2 is:

$$d^2(\Phi_1, \Phi_2) = \int_\Omega (\Phi_1(\mathbf{x}) - \Phi_2(\mathbf{x}))^2 \, \mathbf{dx}. \tag{2}$$

Other distance measures for implicit shape representations as well as an analysis of their shortcomings can be found in [8]. The distance in (2) reveals a further important advantage of implicit shapes: one can not only measure a discrepancy for given points *on* the contour, but also for all points aside. Thus, matching two embedding functions not only takes the contour into account but also the area of the shapes. For instance the representation in (1) contains the skeleton [3] of the shape. Thus minimizing (2) also seeks to match the skeletons of two shapes. Although the concept carries over to shapes of arbitrary dimension $D \geq 2$, in the following we will focus on the 2-D case.

3.2 Shape Matching with Optic Flow

Matching two shapes respective the distance measure in (2) can be formulated as the minimization over a group of transformations $\mathcal{T}$:

$$E(\mathcal{T}) = \int_\Omega (\Phi_1(\mathbf{x}) - \Phi_2(\mathcal{T}\mathbf{x}))^2 \, \mathbf{dx} \quad \rightarrow \quad \min. \tag{3}$$

The transformations may include, e.g., translation, rotation, and scaling, as in [9], or the group of perspective transformations, as in [19]. In [17] the transformation further comprises arbitrary deformations $\mathbf{w}(\mathbf{x}) := (u(\mathbf{x}), v(\mathbf{x}))^\top$ of the shape, i.e., $\mathcal{T}\mathbf{x} = \mathbf{x} + \mathbf{w}(\mathbf{x})$. As the minimization of (3) yields an ill-posed problem under these conditions, it was suggested to impose a regularization term to the deformation field:

$$E(u, v) = \int_\Omega (\Phi_1(\mathbf{x}) - \Phi_2(\mathbf{x} + \mathbf{w}))^2 + \alpha(|\nabla u|^2 + |\nabla v|^2)\, \mathbf{dx} \tag{4}$$

where $\alpha \geq 0$ is a regularization parameter that steers the influence of the regularization relative to the matching criterion.
In all existing works on shape matching, the minimization of such function(al)s is performed by means of gradient descent. However, this approach has its perfidies: for each optimization variable in (3), one has to choose a step size, and it is not sure, so far, how the step size has to be chosen to ensure convergence. Setting the step size too large can result in severe instabilities depending on the data. A gradient descent on (4), moreover, converges very slowly.
For an alternative numerical scheme, we suggest to make use of recent advances in optic flow estimation. Optic flow generally describes the 2-D motion field between images, and (4) is a well-known functional for computing optic flow. When regarding Φ_1 and Φ_2 as gray scale images, the estimation of the shape deformation field $\mathbf{w}$ yields an optic flow estimation problem. The first term in (4) contains the non-linearized optic flow constraint, which, in this case, implements the constraint that $\mathbf{w}(\mathbf{x})$ matches points with the same distance to the contour. The second term is a regularizer that penalizes variations in the flow field. This means, in particular, that there should be as few deformations as possible and the deformation field is sought to be smooth.
It has been shown in [5] that the minimization of such a nonlinear functional can be performed by solving a sequence $k = 0, ..., n$ of linear systems

$$\begin{aligned} \left(\Phi_x^k du^k + \Phi_y^k dv^k + \Phi_z^k\right) \Phi_x^k - \alpha\Delta(u^k + du^k) = 0 \\ \left(\Phi_x^k du^k + \Phi_y^k dv^k + \Phi_z^k\right) \Phi_y^k - \alpha\Delta(v^k + dv^k) = 0 \end{aligned} \tag{5}$$

with $\mathbf{w}^0 = 0$, $\mathbf{w}^{k+1} = \mathbf{w}^k + (du^k, dv^k)^\top$, the abbreviations $\Phi_x^k := \partial_x \Phi_2(\mathbf{x} + \mathbf{w}^k)$, $\Phi_y^k := \partial_y \Phi_2(\mathbf{x} + \mathbf{w}^k)$, $\Phi_z^k := \Phi_2(\mathbf{x} + \mathbf{w}^k) - \Phi_1(\mathbf{x})$, and $\Delta = \partial_{xx} + \partial_{yy}$ the Laplace operator. Note that in comparison to the more general functional in [5], the terms in (4) are both quadratic. Consequently, the inner fixed point iteration loop performed in [5] is not necessary. Quadratic terms for both the matching and the smoothness constraints are sufficient for the matching problem here, since there is basically no noise in Φ_1 and Φ_2 and discontinuities in the deformation field $\mathbf{w}$ are not desired. Robust non-quadratic regularizers or matching terms do not appear to be necessary but are conceivable.
This numerical scheme does not rely on a gradient descent. The linear systems in (5) are the outcome of a semi-implicit scheme that does not introduce a time step size. For solving the linear systems, one can employ iterative solvers such as Gauss-Seidel or SOR. These solvers always converge under the given

conditions, independent from the data, and they converge much faster than a comparable gradient descent. A multi-resolution implementation as in [5] leads to an additional speedup and real-time performance (13 frames/sec with non-optimized C++ code on a 2GHz Laptop and 219×132 images). In the sequel, we will compare this optic flow based shape matcher with the ICP algorithm.

4 An Application: Silhouette Based 2-D-3-D Pose Estimation

We test the two shape matching methods in the context of contour based 2-D-3-D pose estimation. In this application, a known 3-D surface model (we use a tea pot here) is projected to the image plane to yield the object silhouette there. This silhouette is compared via shape matching to the contour extracted from the image by a segmentation method. This yields correspondences between points from the model silhouette to points from the contour, which are then used for a pose update. A summary of the algorithm is as follows:

1. **Surface projection**: project the surface with the initial pose to the image plane.
2. **Contour extraction**: segment the object region in the image.
3. **Shape matching**: register the two shapes by either ICP or optic flow.
4. **Pose update:** use the point correspondences from the matching for a pose update.
5. **Iterate:** repeat step 1 to 4 until convergence.

Point correspondences stemming from different camera views can be easily consolidated in step 4. For a detailed description of the method we refer to [6]. The critical issue, apart from the segmentation, is the shape matching. It is important that the matching can cope with noisy shapes due to segmentation errors as well as deformations due to 3-D rotations. In the following section, the performance of ICP as well as optic flow based point correspondences is evaluated. We also tested the simultaneous usage of correspondences from both matchers: Since both algorithms provide a set of 2D-3D correspondences, in step 4 they can be used together and solved simultaneously.

5 Experiments

We first analyzed the influence of the shape matching method on the accuracy and stability of the pose estimation when the images are disturbed by noise, partial occlusions, or changing lighting conditions. To this end, we used a stereo sequence consisting of 350 frames, to which we added Gaussian noise with a standard deviation of up to 80. Some sample frames without noise are shown in Fig. 2. During the whole sequence the object is not moving, thus, it is possible to regard the pose variance for a quantitative analysis. Note that the pose estimation method is able to capture moving objects, as well, as shown in a further experiment. The parameters were not tuned for the specific sequence.

Fig. 2. Some frames from a static stereo sequence (350 frames) with illumination changes and partial occlusions. **Top row:** left view. **Bottom row:** right view.

The diagrams in Fig. 3 show the deviation from the mean pose when the method employed ICP, optic flow (OF), or their combination for matching (ICP+OF). Obviously, ICP provides a slightly more stable pose than the matching with optic flow. This can also be conjectured from Table 1 that lists the variances for the three matchers and different levels of noise. One can also see that the combination of point correspondences from both matching methods yields similar results as ICP alone. Figure 4 shows two example frames of the sequence. The pose is overlaid in the images.

Noise	Matcher	R_x	R_y	R_z	T_x	T_y	T_z
0	ICP+OF	0.0004	0.00009	0.00009	0.97	0.54	1.25
0	OF	0.0005	0.00017	0.00017	1.64	0.61	2.31
0	ICP	0.0007	0.0005	0.000045	1.39	0.6	1.84
40	ICP+OF	0.0005	0.00013	0.00013	1.79	0.31	1.76
40	OF	0.001	0.00034	0.000355	5.01	0.32	6.4
40	ICP	0.0003	0.0001	0.00009	0.96	0.48	1.49
80	ICP+OF	0.0004	0.0002	0.00019	2.29	0.53	2.16
80	OF	0.0069	0.00036	0.00036	4.58	0.57	5.08
80	ICP	0.00048	0.0002	0.0002	2.18	0.79	2.44

Table 1. Variances of the pose parameters (rotation, translation) for different matchers and noise levels (Gaussian noise with standard deviation 0, 40, and 80). The rotations are given in radians and the translations in millimeters.

While the first experiment evaluated the matchers in a situation where the shapes are already close to each other, in the second experiment, we tested the performance, when the model silhouette is far from the object contour in the images. For this purpose, we computed the contours as well as the pose in the first frame of the sequence as usual. We then disturbed the object's pose by a rotation in

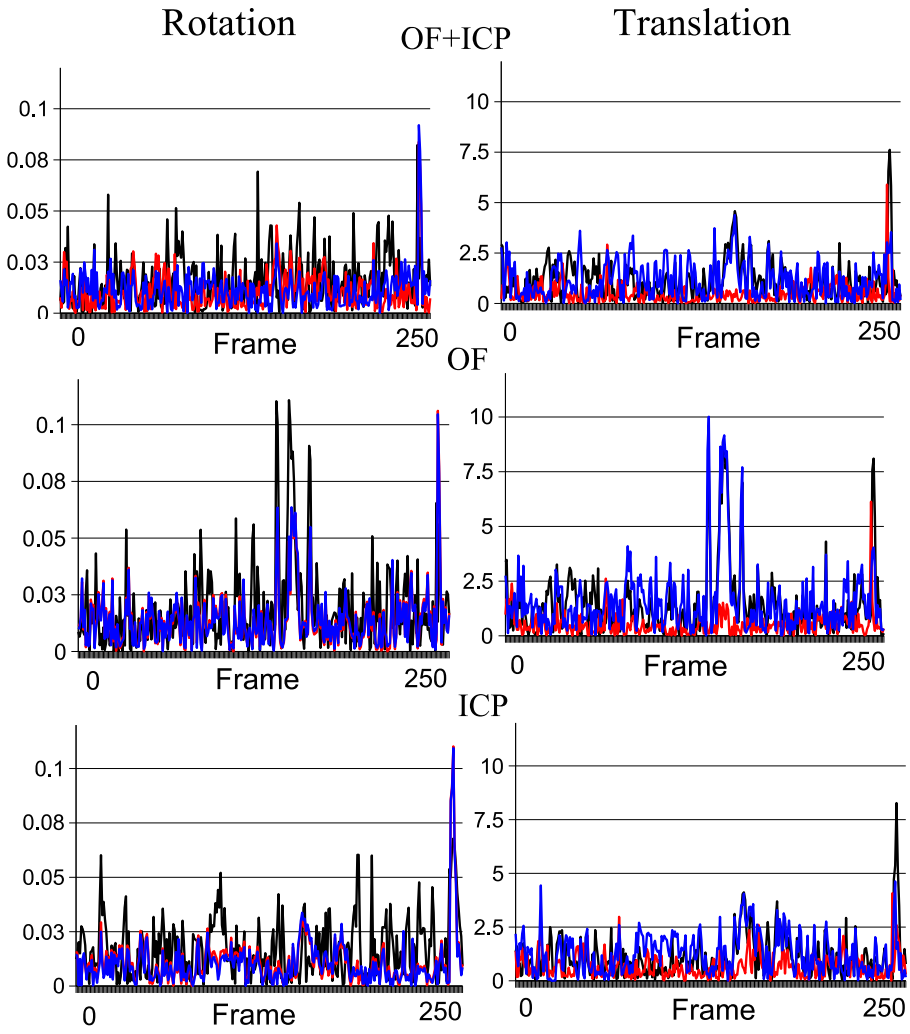

Fig. 3. Deviations from the mean pose for rotation (along the x, y and z-axes in radians) and translation (along the x, y and z-axes in mm) when the method uses the matching with optic flow, ICP, or the combination of both, respectively.

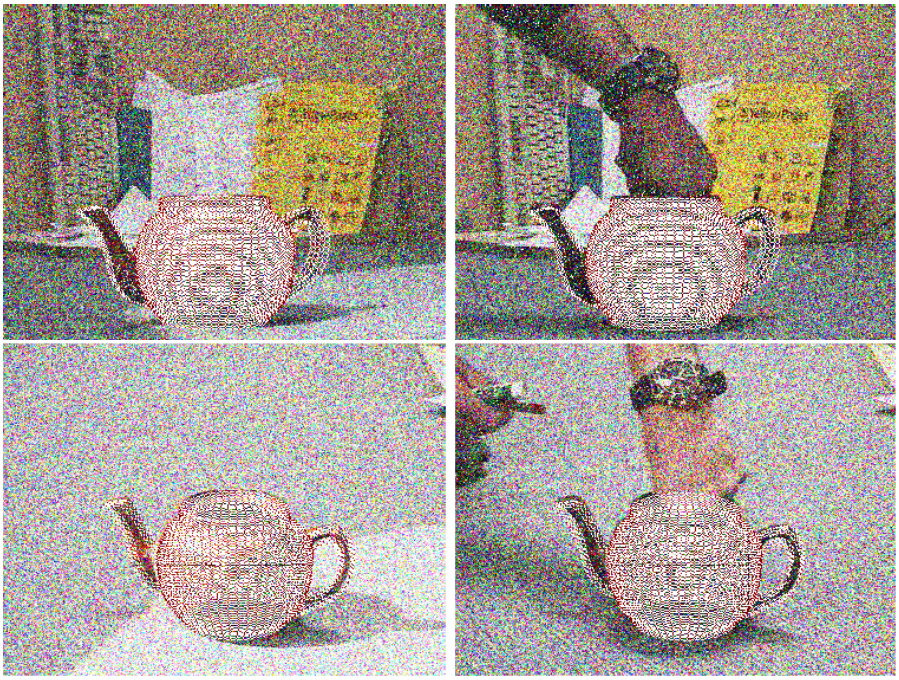

Fig. 4. Two exemplary pose results for the sequence with heavy noise.

the area of $[-60 \dots 60]$ degrees around the x, y, and z axes, or a translation in the area of $[-150 \dots 150]$ mm along these axes. We generated 1000 samples in these intervals. Fig. 5 depicts for which rotations and translations the method was able (blue stars) or not able (red crosses) to converge back to the initially estimated pose. For an absolute translational deviation of less than 3mm, the pose was counted as converged, otherwise as failure. Obviously, the ICP matcher has more problems in case of large transformations than the optic flow based matcher. Combining both matchers yields a similar performance as for the optic flow matcher. Fig. 6 shows some exemplary rotations for which the method with the OF-ICP matcher converged, but the method using the plain ICP-algorithm did not. Table 2 summarizes the convergence rates in percent.

Matcher	Rotation	Translation
ICP+OF	51.4 %	50.1 %
OF	55.7 %	46.7 %
ICP	27.8 %	32.9 %

Table 2. The convergence rate for the second experiment (see Fig. 5) in percent.

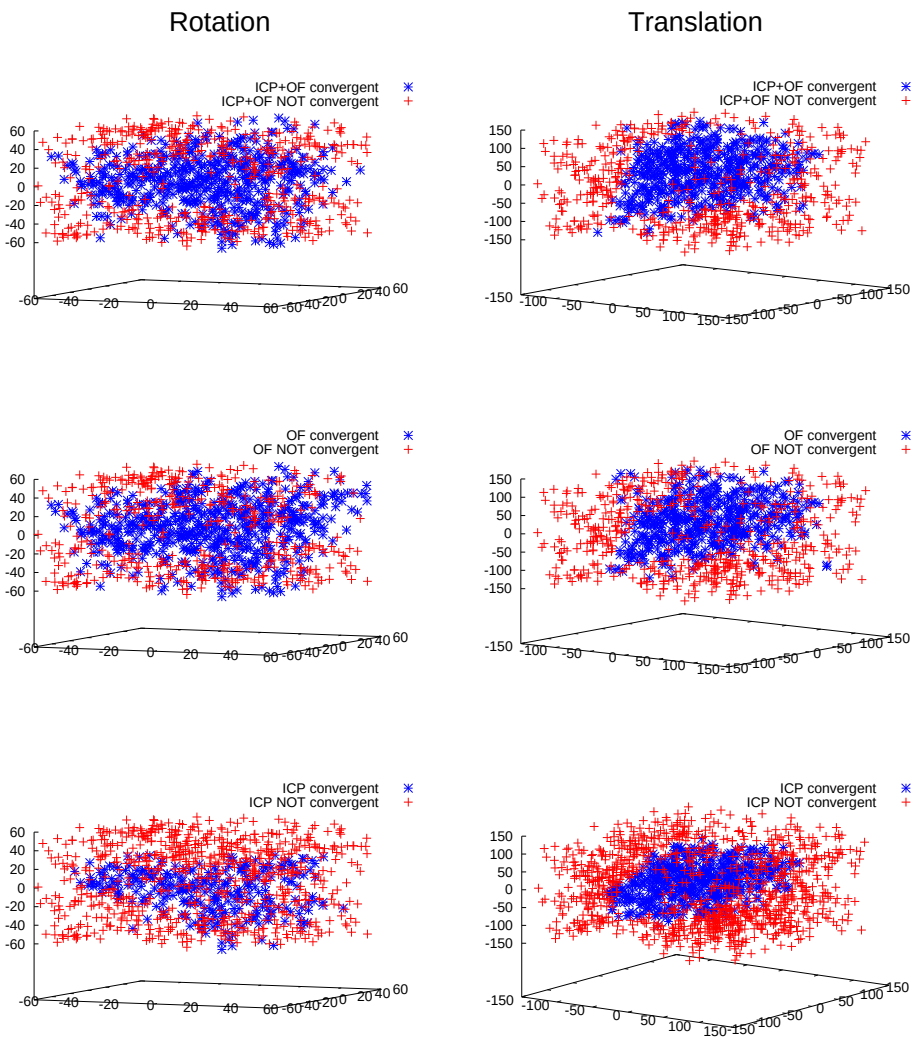

Fig. 5. Convergence of the three investigated methods for the same 1000 random disturbances in rotation (left) and translation (right). Blue stars show the disturbances for which the algorithm was able to converge back to the correct pose, red crosses show the cases of failure. The methods using the combination of ICP and optic flow (top) or solely the optic flow (middle) reveal a similar performance that is significantly better than the performance using the ICP algorithm alone (bottom).

Fig. 6. Example rotations, which still converged using the ICP+OF algorithm but failed with ICP alone.

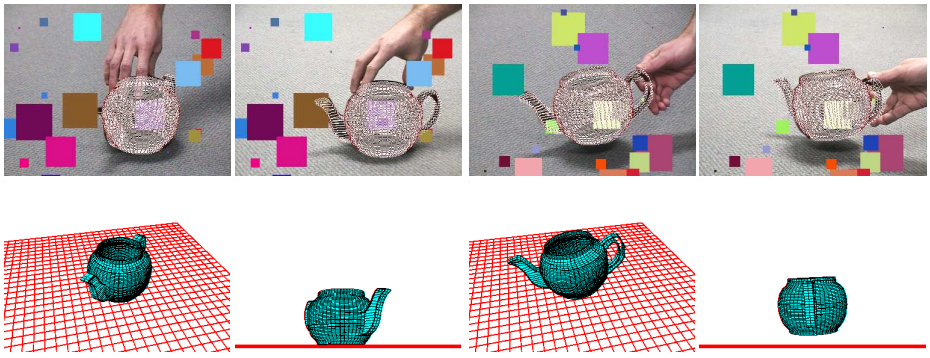

Fig. 7. A second stereo sequence where the object is moved (345 frames). The handle of the tea pot temporarily vanishes behind the container and reappears. Finally the tea pot is moved around. **Top:** Pose results for different frames. **Bottom:** Synthetic visualization of the object and the estimated pose from different perspective views.

According to the literature, as a rough rule for convergence, rotations must be below 20 degrees [7]. This is approximately the convergence radius we also obtained for ICP. Obviously, with the optic flow matcher, the convergence radius can be significantly larger (up to 40 degrees). A possible explanation for this outcome is the richer description of a shape by means of the signed distance function. This includes area based properties of a 2-D shape, which help in the usually ill-posed problem of fitting a 3-D surface to its projections in the image.

Finally, Fig. 7 shows pose results of a second stereo sequence, in which the tea pot is grabbed and moved around. We artificially distorted the images by overlaying rectangles of random size, position and color. The bottom row shows pose results in a virtual environment. Also for this sequence, we show a tracking diagram in Fig. 8. It compares the estimated x- y- and z-axis of the estimated pose for different matching strategies (ICP+OF, OF, and ICP). Furthermore,

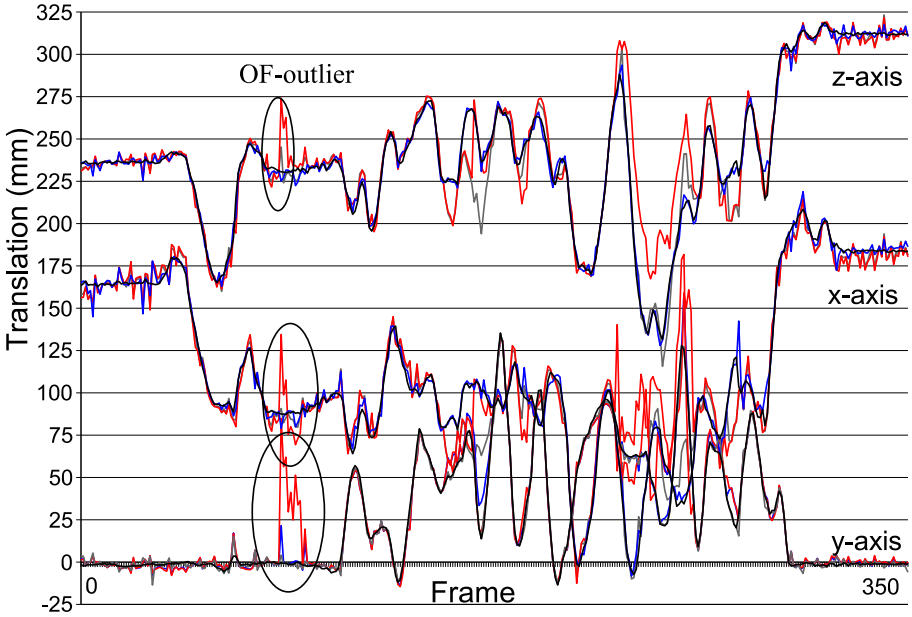

Fig. 8. Visualization of the x, y and z-axis while tracking the sequence in Fig. 7. The values show the results of the OF (red), ICP (gray), and ICP+OF (blue) matcher for the artificially distorted images. Furthermore, the result for the non-distorted images and the ICP+OF matcher is overlaid (black). All diagrams show a similar behavior, except for the OF matcher, which is more sensitive to this kind of distortion.

we overlaid the result of the non-distorted sequence (which can be regarded as rough ground truth).
The distortions lead to errors in the pose estimation. With the ICP and ICP+OF matching these errors are mainly within a range of a few millimeter. Solely the results of the plain OF-approach show significantly larger errors in some parts of the sequence. One such part is indicated in the diagram. Obviously, the OF matcher is more sensitive to this kind of distortion than the ICP approach. This is because the distance function propagates the errors in the contour, whereas the ICP approach often ignores smaller occlusions by always taking the closest point for matching. Nonetheless, the combined ICP+OF approach still shows a stable tracking behavior.

6 Conclusions

Two very different shape matching concepts have been investigated, one based on explicitly given contour points and another based on implicit shape representations via level sets. We have shown that matching shapes in the level set framework can be performed efficiently with a numerical scheme known from

optic flow estimation. Moreover, we compared an ICP algorithm on an explicit contour representation and the level set based matching in the context of silhouette based 3-D pose estimation. It turned out that ICP on explicit contours yields estimates with less variations, whereas the optic flow matcher on the level set representation shows a clearly better convergence in case of large transformations. With the possibility to combine results from both matchers in the pose estimation framework, we demonstrated that one can obtain the best of both registration methods.

References

1. R. Bergevin, M. Soucy, H. Gagnon, and D. Laurendeau. Towards a general multiview registration technique. *IEEE Transactions on Pattern Analysis and Machine Intelligence*, 18(8):540–547, 1996.
2. P. Besl and N. McKay. A method for registration of 3D shapes. *IEEE Transactions on Pattern Analysis and Machine Intelligence*, 12:239–256, 1992.
3. H. Blum. A transformation for extracting new descriptors of shape. In W. Wathen-Dunn, editor, *Models for the Perception of Speech and Visual Form*, pages 362–380. MIT Press, 1967.
4. R. W. Brockett and P. Maragos. Evolution equations for continuous-scale morphology. In *Proc. IEEE International Conference on Acoustics, Speech and Signal Processing*, volume 3, pages 125–128, San Francisco, CA, Mar. 1992.
5. T. Brox, A. Bruhn, N. Papenberg, and J. Weickert. High accuracy optical flow estimation based on a theory for warping. In T. Pajdla and J. Matas, editors, *Computer Vision - Proc. 8th European Conference on Computer Vision*, volume 3024 of *LNCS*, pages 25–36. Springer, May 2004.
6. T. Brox, B. Rosenhahn, and J. Weickert. Three-dimensional shape knowledge for joint image segmentation and pose estimation. In W. Kropatsch, R. Sablatnig, and A. Hanbury, editors, *Pattern Recognition*, volume 3663 of *LNCS*, pages 109–116. Springer, Aug. 2005.
7. D. Chetverikov, D. Stepanov, and P. Krsek. Robust Euclidean alignment of 3D point sets: The trimmed iterative closest point algorithm. *Image and Vision Computing*, 23(3):299–309, 2005.
8. D. Cremers and S. Soatto. A pseudo distance for shape priors in level set segmentation. In O. Faugeras and N. Paragios, editors, *Proc. 2nd IEEE Intl. Workshop on Variational, Geometric and Level Set Methods (VLSM)*, pages 169–176, 2003.
9. D. Cremers, N. Sochen, and C. Schnörr. Multiphase dynamic labeling for variational recognition-driven image segmentation. In T. Pajdla and J. Matas, editors, *Proc. 8th European Conference on Computer Vision*, volume 3024 of *LNCS*, pages 74–86. Springer, Berlin, May 2004.
10. A. Dervieux and F. Thomasset. A finite element method for the simulation of Rayleigh–Taylor instability. In R. Rautman, editor, *Approximation Methods for Navier–Stokes Problems*, volume 771 of *Lecture Notes in Mathematics*, pages 145–158. Springer, Berlin, 1979.
11. J. Feldmar and N. Ayache. Rigid, affine and locally affine registration of free-form surfaces. *International Journal of Computer Vision*, 18:99–119, 1996.
12. P. F. Felzenszwalb and D. P. Huttenlocher. Distance transforms of sampled functions. Technical Report TR2004-1963, Computer Science Department, Cornell University, Sept. 2004.

13. A. E. Johnson and S. B. Kang. Registration and integration of textured 3-D data. In *Proc. International Conference on Recent Advances in 3-D Digital Imaging and Modeling*, pages 234–241. IEEE Computer Society, May 1997.
14. L. J. Latecki and R. Lakämper. Shape similarity measure based on correspondence of visual parts. *IEEE Transactions on Pattern Analysis and Machine Intelligence*, 22(10):1185–1190, Oct. 2000.
15. M. E. Leventon, W. E. L. Grimson, and O. Faugeras. Statistical shape influence in geodesic active contours. In *Proc. 2000 IEEE Computer Society Conference on Computer Vision and Pattern Recognition (CVPR)*, volume 1, pages 316–323, Hilton Head, SC, June 2000.
16. S. Osher and J. A. Sethian. Fronts propagating with curvature-dependent speed: Algorithms based on Hamilton–Jacobi formulations. *Journal of Computational Physics*, 79:12–49, 1988.
17. N. Paragios, M. Rousson, and V. Ramesh. Distance transforms for non-rigid registration. *Computer Vision and Image Understanding*, 23:142–165, 2003.
18. X. Pennec and J. Thirion. A framework for uncertainty and validation of 3D registration methods based on points and frames. *International Journal of Computer Vision*, 25(3):203–229, 1997.
19. T. Riklin-Raviv, N. Kiryati, and N. Sochen. Unlevel-sets: geometry and prior-based segmentation. In T. Pajdla and J. Matas, editors, *Proc. 8th European Conference on Computer Vision*, volume 3024 of *LNCS*, pages 50–61. Springer, Berlin, May 2004.
20. B. Rosenhahn. *Pose Estimation Revisited*. PhD thesis, University of Kiel, Germany, Sept. 2003.
21. B. Rosenhahn and G. Sommer. Pose estimation of free-form objects. In T. Pajdla and J. Matas, editors, *Computer Vision - Proc. 8th European Conference on Computer Vision*, volume 3021 of *LNCS*, pages 414–427. Springer, May 2004.
22. S. Rusinkiewicz and M. Levoy. Efficient variants of the ICP algorithm. In *Proc. 3rd Intl. Conf. on 3-D Digital Imaging and Modeling*, pages 224–231, 2001.
23. K. Siddiqi, A. Shokoufandeh, S. Dickinson, and S. Zucker. Shock graphs and shape matching. *International Journal of Computer Vision*, 35:13–32, 1999.
24. R. Veltkamp and M. Hagedoorn. State-of-the-art in shape matching. Technical Report UU-CS-1999-27, Utrecht University, Sept. 1999.
25. Z. Zhang. Iterative points matching for registration of free form curves and surfaces. *International Journal of Computer Vision*, 13(2):119–152, 1994.